Crystallization kinetics of rapidly quenched $Cu_{50}Zr_{50}$ and $Cu_{46}Zr_{46}Al_8$ glass-forming alloys

T V Kulikova[1], A A Ryltseva[1], V A Bykov[1,2], S Kh Estemirova[1,2] and K Yu Shuhyaev[1,2]

[1]Institute of Metallurgy, Ural Branch of Russian Academy of Sciences, Ekaterinburg, Russia
[2]Ural Federal University named after First President of Russia B.N. Yeltsin, Ekaterinburg, Russia

E-mail: kuliko@gmail.com

Abstract. We studied the crystallization processes, the structure and thermal properties of amorphous alloys $Cu_{50}Zr_{50}$ and $Cu_{46}Zr_{46}Al_8$ in a wide temperature range. Comparative study of the crystallization kinetics of these amorphous alloys was carried out for the first time using multivariate non-linear regression. It was found that mechanisms of the crystallization of studied metallic glasses are substantially different. The binary alloy is crystallized by branched reaction complex in four steps. For the ternary system was proposed two-step kinetic model of the crystallization process with consecutive reactions. The values of the total energy of activation for each crystallization stage reach to $Cu_{50}Zr_{50}$: E_1 (345.2 kJ/mol); E_2 (307.9 kJ/mol), E_3 (281.1 kJ/mol), E_4 (259.51 kJ/mol) and $Cu_{46}Zr_{46}Al_8$: E_1 (350.7 kJ/mol); E_2 (150.4 kJ/mol).

1. Introduction

The Cu-Zr system has unique glass-forming ability (GFA) and so it is the basis for the development of separate class of bulk metallic glasses (BMG) [1-3]. The binary $Cu_{50}Zr_{50}$ alloy, besides the BMG formation, demonstrates shape memory effects due to reversible martensitic transformation. It is well known that small additions of Al essentially improve both the GFA and mechanical properties of binary Cu-Zr alloys [4-7]. In this connection, it is interesting to study the impact of aluminum on the mentioned properties of $Cu_{50}Zr_{50}$ alloy. It was previously found that $Cu_{46}Zr_{46}Al_8$ alloy has the highest GFA among the $(Cu_{0.5}Zr_{0.5})_{100-x}Al_x$ ones [6,8]. So, in this paper we perform comparative study of structure, GFA and crystallization kinetics of binary $Cu_{50}Zr_{50}$ alloy and ternary $Cu_{46}Zr_{46}Al_8$ one.

2. Experimental

The Zirconium, copper and aluminum with purity of 99.98 mass.% were used to pre-pare the Cu-Zr-(Al) alloys with nominal compositions of $Cu_{50}Zr_{50}$ and $Cu_{46}Zr_{46}Al_8$. The initial polycrystalline alloys have been obtained using standard arc-melting technique under helium atmosphere. The initial samples were re-melted at least five times to ensure their homogeneity. The two series of samples were prepared for measurements. The first ones (referred to as as-cast) have been obtained by quenching of the melts on furnace mold with a cooling rate of about 100 K/sec. The samples of the second series (referred to as suction-cast) were obtained by suction casting of the melts into cylindrical copper mould of 2 mm in diameter. The estimated cooling rate in this case was of about 1000 K/s.

The compositions of the alloys as well as the concentrations of impurities were examined by atomic-emission method using the SpectroFlame Modula S analyzer.

X-ray diffraction (XRD) phase analysis and XRD structural analysis were performed using Shimadzu XRD-7000 diffractometer. Phase identification was carried out using PDF-2 database of the ICDD International Centre (The International Centre for Diffraction Data).

Thermal properties of the samples were studied by differential scanning calorimetry (DSC) during heating at different rates using a Netzsch STA 449C calorimeter. Kinetic analysis was performed with Thermokinetics Netzsch-Gerätebau GmbH software.

3. Results and discussion

Firstly, we compare the structure and crystallization process of as-cast and suction-cast samples for both the $Cu_{50}Zr_{50}$ and $Cu_{46}Zr_{46}Al_8$ alloys. In Fig.1 the XRD patterns for all the samples mentioned are shown. It can be seen that as-cast $Cu_{50}Zr_{50}$ alloy is the mixture of two monoclinic martensitic phases $P2_1/m$ and Cm (see Fig.1a). The XRD peaks are rather broad due to the high density of the defects caused by the existence of martensitic phases. The suction-cast $Cu_{50}Zr_{50}$ sample is mostly amorphous but small amounts of both B2 and B19' modifications of CuZr intermetallic compounds are present (Fig.1b). So, the sample may be treated as composite of the amorphous matrix with CuZr phase embedded. The XRD pattern for as-cast $Cu_{46}Zr_{46}Al_8$ alloy is a broad amorphous-like hump with the single pronounced crystalline peak corresponding to B2 CuZr phase (Fig1c). The suction-cast sample of this alloy is X-ray amorphous (Fig1d).

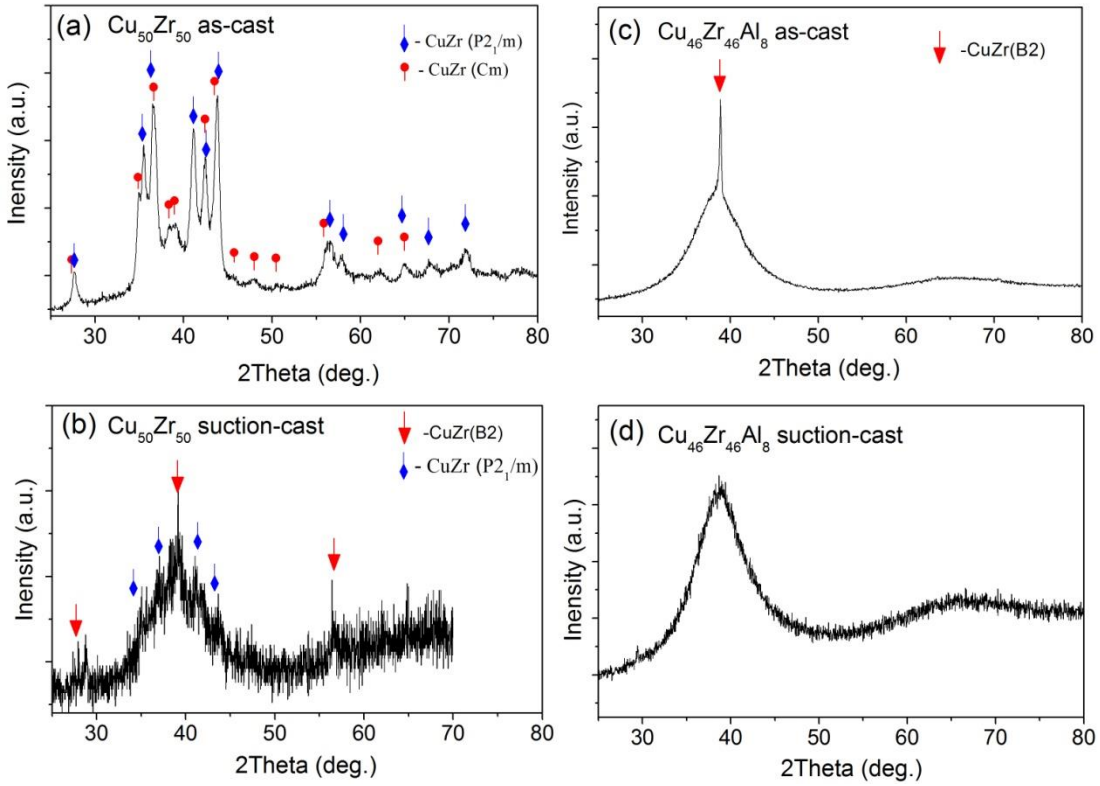

Figure 1. XRD patterns for binary $Cu_{50}Zr_{50}$ alloy (a,b) and triple $Cu_{46}Zr_{46}Al_8$ one (c,d) obtained for the as-cast (a,c) and suction-cast (b,d) samples.

The results of XRD analysis are confirmed by calorimetric measurements (Fig. 2). Indeed, the DSC curve of as-cast $Cu_{50}Zr_{50}$ sample shows the absent of amorphous phase. Instead we see austenitic (reverse martensitic) transformation (A_s) at T= 523 K and then the decomposition (T = 870 K) and formation (T = 1000 K) of CuZr B2 phase, respectively. The temperature of B2 phase formation is in accordance with phase diagram of Cu-Zr system [9]. The DSC curve of suction-cast $Cu_{50}Zr_{50}$ sample demonstrates a kink at the glass transition temperature T_g = 650 K and two peaks at T_1 = 710 K and T_2

= 750 K corresponding to crystallization process. The peculiarities of the latter will be described below.

DSC curves obtained for as-cast and suction-cast $Cu_{46}Zr_{46}Al_8$ samples are very similar (Fig.2b). A small difference between the transition temperatures is only observed. So we conclude that obtained XRD and DSC data are in close agreement with each other.

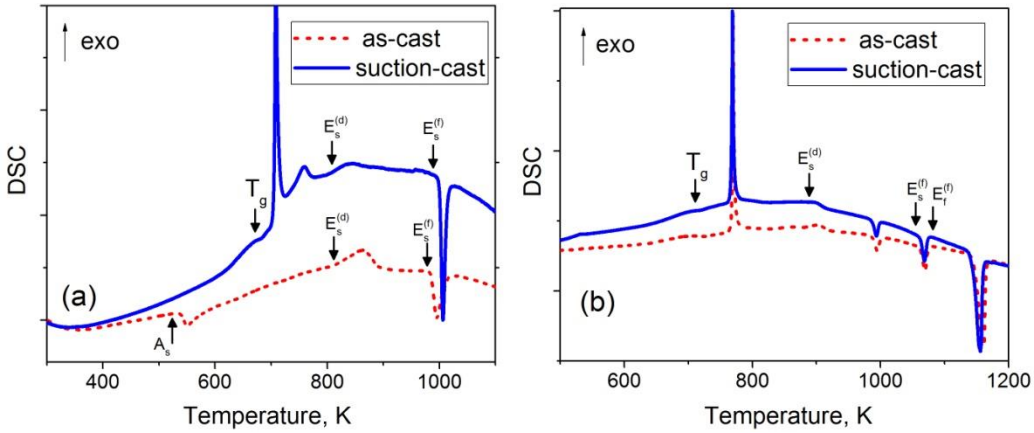

Figure 2. DSC curves for $Cu_{50}Zr_{50}$ (a) and $Cu_{46}Zr_{46}Al_8$ (b) alloys. The (red) dashed and (blue) solid lines correspond to as-cast and suction-cast samples, respectively. A_s - austenitic (reverse martensitic) transformation; $E_s^{(d)}$ – onset of eutectoid decomposition; $E_s^{(f)}$ – onset of eutectoid formation; $E_f^{(f)}$ - end of eutectoid formation; T_g - glass transition temperature.

In order to study the crystallization kinetics in the systems under investigation, we have performed DSC measurements of suction cast samples heating them from 300 K up to 823 K at different heating rates. The DSC data have been described by non-linear regression method with using Thermokinetics Netzsch-Gerätebau GmbH software. Verification of kinetic analysis data has been performed by both XRD and thermodynamic data obtained in [11,12].

The $Cu_{50}Zr_{50}$ sample has been heated at the rates of 1, 2, 4 and 8 K/min (see Fig. 3). During the kinetic analysis of a process, the optimal kinetic model describing the sequence of chemical reaction in the system under investigation is constructed [13]. For the $Cu_{50}Zr_{50}$ suction-cast alloy, the best model obtained is:

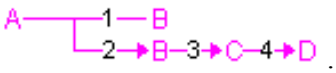

Here both the reaction $A \rightarrow B$ (1 and 2) correspond to the formation of CuZr B2 phase and obeys the extended Prout-Tompkins autocatalytic reaction equation:

$$\frac{d\alpha}{dt} = -k\alpha^n \beta^m . \qquad (1)$$

Hereinafter $k = k(T) = A\exp(-E_a / RT)$ is the reaction rate constant which obeys the Arrhenius law; α is the concentration of an initial component; β the concentration of a reaction product; t is the time and T is the temperature. The catalyst of the reaction is the CuZr B2 phase which is present in amorphous matrix. The reaction $B \rightarrow C$ (3) corresponds to the transformation $CuZr \rightarrow CuZr_2 + Cu_{10}Zr_7$ taking place in the form of dissusion-limited reaction obeying the Fik's law. In this case, the time dependence of reaction conversion is described by interpolation formula obtained from a solution of boundary-value problem for diffusion equation [14]. The transformation $C \rightarrow D$ (4) probably

corresponds to re-crystallization of equilibrium phases $CuZr_2$ and $Cu_{10}Zr_7$ and proceeds as n-order autocatalytic reaction:

$$\frac{d\alpha}{dt} = -k\alpha^n(1+k_{cat}\beta), \tag{2}$$

where k_{cat} is the coefficient of autocatalysis.

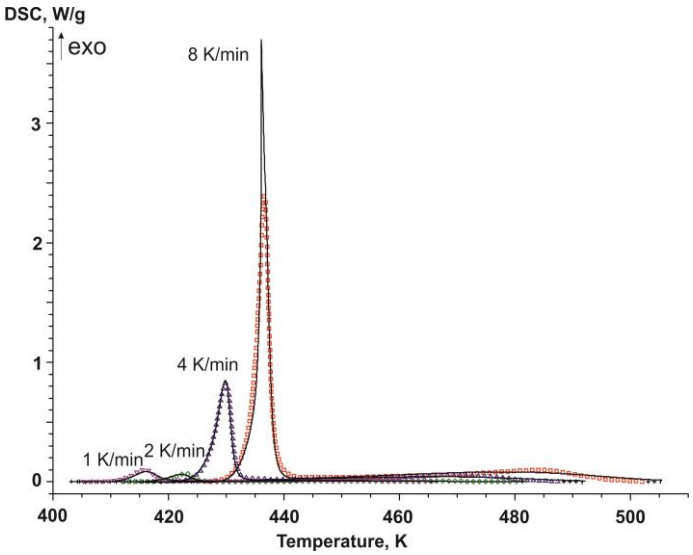

Figure 3. Thermograms of suction-cast $Cu_{50}Zr_{50}$ sample at different heating rates. Dotted and solid lines represent experimental data and the results of kinetic analysis, respectively.

The suction-cast $Cu_{46}Zr_{46}Al_8$ sample has been heated at the rates of 2, 4 and 8 K/min (see Fig. 4). Experimental DSC curves have been optimally described by the reaction sequence:

A—1→B—2→C .

The first stage corresponds to nucleation and growth which is described by classical Avrami model:

$$\frac{d\alpha}{dt} = -k\alpha(-\ln\alpha)^{\frac{n-1}{n}} \tag{3}$$

where, n is the parameter depending on both the nucleus geometry and their growth mechanism [15]. The second stage corresponds to n-order reaction:

$$\frac{d\alpha}{dt} = -k\alpha^n . \tag{4}$$

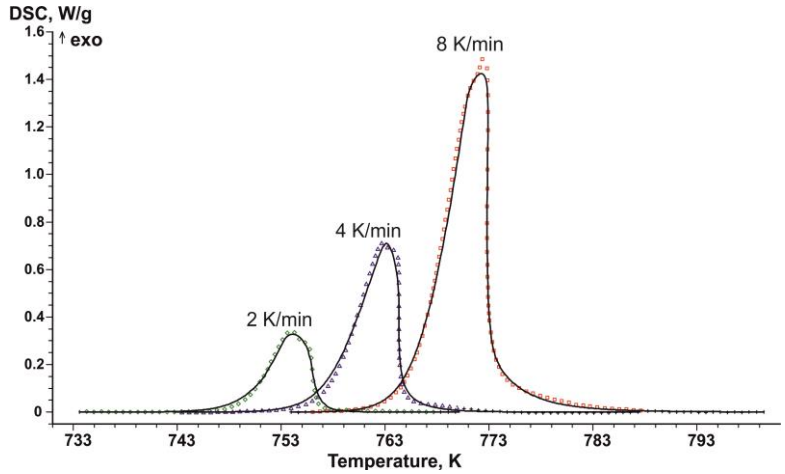

Figure 4. Thermograms of suction-cast $Cu_{46}Zr_{46}Al_8$ sample at different heating rates. Dotted and solid lines represent experimental data and the results of kinetic analysis, respectively.

The interpretation of the proposed reactions for $Cu_{46}Zr_{46}Al_8$ alloy is complicated due to the absence of both an accepted phase diagram of Cu-Zr-Al system and reliable high-temperature XRD data. In accordance with assessed phase diagram of Cu-Zr-Al system [12], the equilibrium state of the $Cu_{46}Zr_{46}Al_8$ alloy, at the temperatures in the vicinity of the crystallization DSC peak, is the mixture of three phases: $Cu_{10}Zr_7$, $CuZr_2$ и $AlCu_2Zr$. So we guess that the first reaction $A \rightarrow B$ corresponds to the formation of equilibrium phases and some metastable one; the second stage $B \rightarrow C$ is the formation of equilibrium phases $Cu_{10}Zr_7$, $CuZr_2$ и $AlCu_2Zr$. An additional study is needed to confirm this hypothesis.
The activation energies E_a and pre-exponent factors A, obtained from kinetic analysis are presented in Table 1.

Table 1. Kinetic parameters of crystallization of $Cu_{50}Zr_{50}$ and $Cu_{46}Zr_{46}Al_8$ amorphous alloys.

Sample	**E_A, kJ/mol**				**log A, s^{-1}**			
	1	2	3	4	1	2	3	4
$Cu_{50}Zr_{50}$	345.2	307.9	281.1	259.5	24.6	22.7	18.8	15.8
$Cu_{46}Zr_{46}Al_8$	350.7	150.4	-	-	19.4	9.7	-	-

4. Conclusions

The comparison of crystallization kinetics of $Cu_{50}Zr_{50}$ and $Cu_{46}Zr_{46}Al_8$ amorphous alloys has been carried out for the first time with using non-linear kinetic modeling. It has been found that mechanisms of crystallization of the systems under consideration are essentially different. The binary alloy crystallizes through the complex branched reaction sequence included autocatalytic reaction and diffusion-limited processes. Whereas, the crystallization of the triple alloy is the sequence of two consecutive reactions described by standard Avrami and n-order reaction equations.

Acknowledgments

The work was supported by Russian Science Foundation (Grant № 14-13-00676).

References

1. Inoue A 2000 *Acta Mater*. **48** 279
2. Inoue A and Zhang W 2004 *Mater.Trans*. **45** 584
3. Son C Y, Kim C K, Shin S Y, Lee S 2009 *Sci. Eng.* **508** 15

4. Lu F, Kong L T, Jiang Z *et al* 2014 *J. Mater. Sci.* **49** 496
5. Wang D, Tan H, Li Y 2005 *Acta Mater*. **53** 2969
6. Zhang Q, Zhang W, Xie G, Inoue A 2007 *Mater. Trans*. **48** (7) 1626
7. Das J, Pauly S, Duhamel C *et al* 2007 *J. Mater. Res.* **22** 326
8. Zhang Q, Zhang W, Inoue A 2007 *Mater. Sci. Forum*. **561-565** 1333
9. Kulikova T V, Bykov V A, Belozerova A A, Murzakaev A M, Ryltsev R E 2013 *J. Non-Cryst. Solids*. **378** 135
10. Zhang S, Ichitsubo T, Yokoyama Y *et al*, 2009 **50** (6) 1340
11. Kalay I, Kramer M J, Napolitano R E 2011 *Metallurg. Mater. Trans.* **42A** 1144-1153.
12. Raghavan V 2011 *J. Phase Equil. Diff.* **32** 452
13. Kulikova T V, Majorova A V, Shunyaev K Yu, Ryltsev R E 2015 *Physica B*. **466–467** 90
14. Serin B and Ellickson R T 1941 *J. Chem. Pys.* **9** 742
15. Liu C, Yu J, Xun S, Zhang J, He J 2003 *Polym. Degrad. Stabil***. 81** 197